Vol. **133** (2018) *ACTA PHYSICA POLONICA A* No. 4

Proceedings of the International Conference on Oxide Materials for Electronic Engineering, May 29–June 2, 2017, Lviv

Manganite Nanoparticles as Promising Heat Mediators for Magnetic Hyperthermia: Comparison of Different Chemical Substitutions

A.I. Tovstolytkin[a,*], Yu.Yu. Shlapa[b], S.O. Solopan[b], A.V. Bodnaruk[c], M.M. Kulyk[c],
V.M. Kalita[c], V.O. Zamorskyi[d], S.M. Ryabchenko[c] and A.G. Belous[b]
[a]Institute of Magnetism of the NAS of Ukraine and MES of Ukraine, 36b Vernadsky Blvd., Kyiv 03142, Ukraine
[b]V.I. Vernadskii Institute of General and Inorganic Chemistry, NAS of Ukraine,
32/34 Palladina Ave., Kyiv 03680, Ukraine
[c]Institute of Physics, NAS of Ukraine, 46 Nauky Ave., Kyiv 03028, Ukraine
[d]Faculty of Radiophysics, Electronics and Computer Systems, Taras Shevchenko National University of Kyiv,
4G Glushkova Ave., Kyiv 03680, Ukraine

Magnetostatic properties and AC magnetic heating characteristics of (La,Sr)MnO_3 nanoparticles with substitutions in manganese and lanthanum sublattices have been studied. The nanoparticles with average sizes in the range 25–38 nm were synthesized via sol–gel method. Fe substitution for Mn, as well as Sm substitution for La have been used in the experiment. It is shown that the increase in substitution level (for both Fe and Sm substitutions) results in lowering the Curie temperature T_C and weakening heating efficiency under the action of AC magnetic field. The results demonstrate that the action of AC field causes effective heating of nanoparticles at temperatures lower than T_C, while heating efficiency becomes strongly reduced at higher temperatures. It is proved experimentally that the substitutions in Mn sublattice result in more rapid changes of magnetic properties, as compared to the substitutions in La one. Thus, complex substitutions based on suitable combinations of substituting elements may serve as an efficient tool to "softly" tune the maximal temperature achieved during the AC magnetic field induced heating of nanoparticles, which is important for application of these materials as heat mediators for self-controlled magnetic nanohyperthermia.

DOI: 10.12693/APhysPolA.133.1017

PACS/topics: magnetic nanohyperthermia, manganite nanoparticles, complex chemical substitutions, Curie temperature, AC magnetic heating characteristics

1. Introduction

Hyperthermia is a rapidly developing technique in cancer therapy [1]. It takes advantage of the higher sensitivity of tumor tissue to heat and typically involves heating of the affected organ to 42–45 °C. Magnetic nanohyperthermia [2] allows minimizing side effects by the localized heating of only desired parts of the organism. The method involves introduction of magnetic nanoparticles (MNPs) into the desired part of the organism and heating them with an AC magnetic field.

Magnetic fluids based on nanocrystalline Fe_3O_4, stabilized by biocompatible surfactants, are typically used as hyperthermia mediators [3]. Unfortunately, due to impossibility to control the local temperature near the particles, there is a risk of overheating and necrosis of normal tissue. This problem could be solved with MNPs of high efficiency of AC magnetic field absorption and a Curie temperature T_C of 42–45 °C. Thus, local temperature control can be ensured even with a nonuniform distribution of mediator particles throughout the tissue, variable magnetic field intensity and uneven dissipation of the evolving heat [4, 5].

Substituted perovskite manganites $La_{1-x}Sr_xMnO_3$ ($x = 0.2$–0.4) are of interest in this context due to easy tunable composition-dependent T_C and relatively large magnetic moment at room temperature [6–8]. The Curie temperature of $La_{1-x}Sr_xMnO_3$ strongly depends on the chemical composition: it displays a maximum at $x \approx 0.3$ ($T_{C_{\max}} \approx 370$ K) and is quite sharply reduced as x deviates from 0.3 [9–11]. A smoother change of the Curie temperature can be reached by additional substitutions either in manganese sublattice [12, 13], or in lanthanum sublattice [14, 15]. Such substitutions are expected to ensure reliable and controllable shift of T_C towards the range, which is necessary for hyperthermia treatment [16].

In this work, the effects of partial substitutions in manganese and lanthanum sublattices on magnetostatic properties and AC magnetic heating characteristics of (La,Sr)MnO_3 MNPs have been studied. Fe substitution for Mn, as well as Sm substitution for La has been used in the experiments. Peculiar features originated from the substitutions in different sublattices have been compared and analyzed.

---

[*] corresponding author; e-mail: atov@imag.kiev.ua

2. Experimental

Iron- and samarium-substituted manganite nanoparticles, $La_{0.77}Sr_{0.23}Mn_{1-x}Fe_xO_3$ with $x_{Fe} = 0$, 0.02, 0.04, 0.06, and $La_{0.7-x}Sm_xSr_{0.3}MnO_3$ with $x_{Sm} = 0$, 0.01, 0.04, 0.06, 0.08, respectively, were synthesized via sol-gel method [17, 18]. Water-soluble salts $La(NO_3)_3$, $Sm(NO_3)_3$, $Sr(NO_3)_2$, $Mn(NO_3)_2$ and $Fe(NO_3)_3$ were used as starting reagents. Necessary molar amounts of raw reagents were dissolved in bidistilled water. Citric acid and ethylene glycol were added as gel-forming additives. The obtained reactive mixture was heated with stirring at 80 °C. The polyesterification reaction took place at pH = 9 and resulted in the formation of a polymer gel. Amorphous powder was obtained after the pyrolysis of the gel at 200 °C. The powder was subjected to further heat treatment at 800 °C for 2 h.

Below, the samples of the first series, $La_{0.77}Sr_{0.23}Mn_{1-x}Fe_xO_3$ with $x_{Fe} = 0$, 0.02, 0.04, and 0.06 will be denoted as Fe00, Fe02, Fe04, and Fe06, respectively. The samples of the second series, $La_{0.7-x}Sm_xSr_{0.3}MnO_3$ with $x_{Sm} = 0$, 0.01, 0.04, 0.06, and 0.08, will be denoted as Sm00, Sm01, Sm04, Sm06, and Sm08, respectively.

X-ray diffraction study (XRD) of the obtained powders was performed using DRON-4 diffractometer (Cu K_α) radiation). Particle size and morphology were studied by transmission electron microscope (TEM) JEOL JEM-1400.

Magnetic measurements were performed using a LDJ-9500 vibrating sample magnetometer. To analyze the field and temperature dependences of magnetization, hysteresis loops were measured for -5 kOe $\leq H \leq 5$ kOe in the temperature range from 110 to 370 K.

To characterize the AC magnetic heating efficiency, magnetic fluids based on synthesized MNPs (50 mg/ml) were prepared using 0.1% aqueous agarose solutions. The fluids were placed into a generator coil, which produced AC magnetic field with a frequency of 300 kHz and amplitude of 120 Oe, and the dependences of the fluid temperature T_{fluid} vs. AC field residence time τ were recorded [19].

3. Results and discussion

According to XRD investigations, all samples are single-phase and crystallize in the distorted perovskite structure. The average nanoparticle sizes lie in the range 25–35 nm for the Fe-substituted series [17] and 31–38 nm for the Sm-substituted one [18].

Magnetic properties of the samples of both series were reported in Refs. [17, 18]. It was shown that both kinds of substitutions (Mn → Fe and La → Sm) give rise to the decrease of room-temperature magnetization and the Curie temperature T_C. The present work emphasizes and discusses the differences in magnetic characteristics originating from substitutions in different sublattices.

Magnetic state of nanoparticles is usually inhomogeneous due to significant contribution of a surface layer whose properties differ from those of the volume properties, and due to the scatter in particle sizes. It was shown in Ref. [17] that temperature behavior of nanoparticles ensemble can be satisfactory described by the introduction of an average Curie temperature T_C concept. It is expected in this case that the behavior of the magnetization of nanoparticles ensemble will obey the law $M(T) \sim \sqrt{T_C - T}$.

Representative temperature dependences of the square of normalized magnetization $m = M(T, H = 5\text{ kOe})/M(110\text{ K}, H = 5\text{ kOe})$ for the Fe- and Sm-substituted samples are shown in the insets of Fig. 1. It is observed that there is a wide temperature range where such dependences are linear (see straight solid lines in the insets). From these dependences, it is possible to estimate the Curie temperature values by the points of intersection of linear area with the temperature axis. For the former series of samples (Fe-substituted ones), T_C monotonically decreases from 343 K to 287 K as x_{Fe} increases from 0 to 0.06. For the Sm-substituted samples, T_C decreases from 376 K to 342 K upon the same rise in x_{Sm}, and then to 324 K as x_{Sm} rises to 0.08.

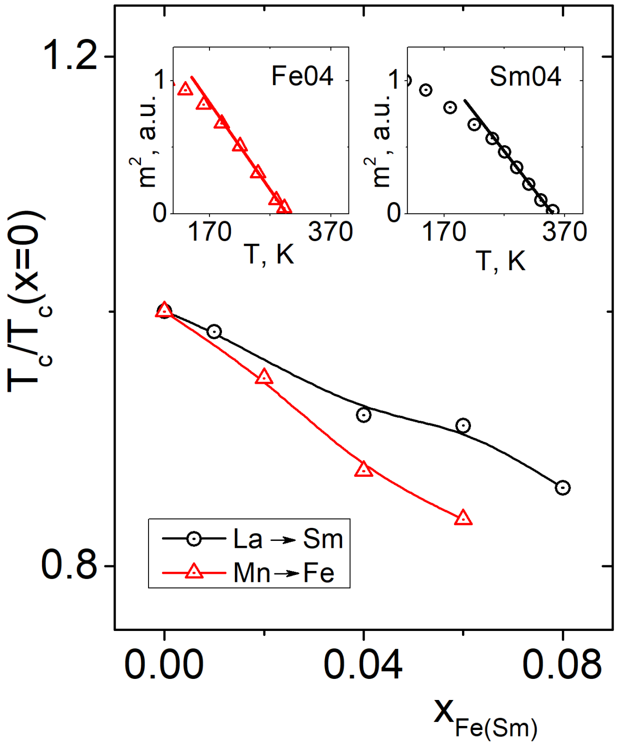

Fig. 1. Concentration dependence of the normalized Curie temperature, $T_C(x)/T_C(x = 0)$, for the Fe- and Sm-substituted samples. Insets show temperature dependences of the square of normalized magnetization $m = M(T, H = 5\text{ kOe})/M(110\text{ K}, H = 5\text{ kOe})$ for Fe04 (left) and Sm04 (right) samples.

Figure 1 compares the relative change of the Curie temperature, $T_C(x)/T_C(x = 0)$, for both series of samples. It is seen that Fe substitution for Mn results in a more rapid change of the Curie temperature: the increase in

x_{Fe} from 0 to 0.06 results in 16% reduction of T_C, while the same rise in x_{Sm} leads only to 9% T_C drop.

The differences between the effects resulted from the substitutions in different sublattices may be explained as follows. Ferromagnetic order in substituted manganites originates from the so-called double exchange interaction between Mn ions which are in different oxidation states (Mn^{3+} and Mn^{4+}) [20]. Earlier, it was shown that Fe ions do not take part in the double exchange [12, 13, 21]. As a result, Fe substitution for Mn simply reduces the number of Mn ions participating in the double exchange. On the contrary, Sm substitution for La does not affect the quantity and oxidation state of Mn ions. Instead, it weakens inter-ionic interactions by means of introduction and subsequent enhancement of local distortions of crystalline structure [15, 22], because the ionic radius of Sm^{3+} is smaller than that of La^{3+} [18].

Based on the obtained nanoparticles and aqueous agarose solution, magnetic fluids were prepared for the investigation of the AC magnetic heating efficiency. Insets of Fig. 2 show representative T_{fluid} vs. τ dependences for the Fe- and Sm-substituted samples measured after the field with a frequency of 300 kHz and amplitude of 120 Oe was turned on. It is established that all samples heat up effectively under the action of AC magnetic field, however, the ability to be heated decreases with $x_{Fe(Sm)}$ growing.

It is known that magnetic nanoparticles, being placed in an AC magnetic field, can dissipate the energy to the surrounding environment due to the viscous particle rotation (the Brown mechanism) or magnetization reversal (either the Néel–Brown relaxation mechanism, or hysteresis processes which are usually described on the basis of the Stoner–Wohlfarth model) [23]. It was shown in Ref. [24] that for the manganite nanoparticles with the sizes of 25–40 nm, the dominant heating mechanism is hysteretic processes of magnetization reversal. In this case, the heating efficiency depends on the saturation magnetization, coercivity, and shape of the hysteresis loop. In our case, the main cause of the reduced heating efficiency in the samples with higher Fe (Sm) content is believed to be strong reduction of saturation magnetization with the increase in $x_{Fe(Sm)}$ [17, 18].

It is important that after the abrupt initial temperature rise (observed after turning on AC magnetic field), each curve in the insets of Fig. 2 reaches a saturation at a certain temperature T_s. Figure 2 compares T_s/T_C values for both series of samples. It is seen that the T_s/T_C ratio is close to 1 for all samples under study. However, it should be noted that T_s is not always exactly equal to T_C, since T_s depends not only on the magnetic parameters of nanoparticles, in particular on a scatter in the values of magnetization and the Curie temperature, but also on the features of heat exchange with environment.

It may be concluded from Fig. 1 and insets of Fig. 2 that the substitutions in Mn sublattice result in more rapid changes of T_C and T_s, as compared to the substitutions in La one. Thus, complex substitutions based on suitable combinations of substituting elements are expected to be able to ensure a reliable and controllable shift of T_s towards the range, which is necessary for magnetic hyperthermia or other applications.

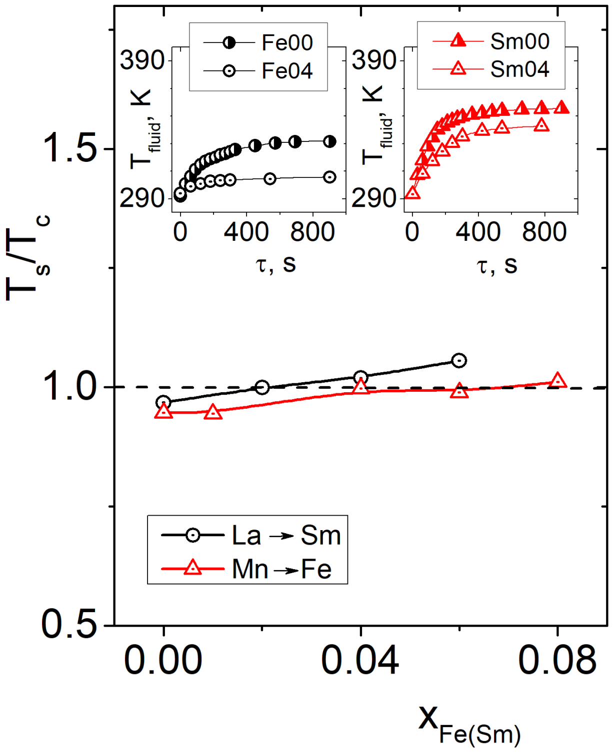

Fig. 2. Concentration dependences of the ratio of T_s/T_C for the fluids based on Fe- and Sm-substituted samples (here, T_s is the temperature of maximal heating under AC magnetic field (frequency of 300 kHz and amplitude of 120 Oe) and T_C is the Curie temperature). Insets show representative T_{fluid} vs. τ dependences for Fe00 and Fe04 samples (left) and Sm00 and Sm04 ones (right), measured after AC field with the above parameters turned on.

Based on the results of investigations, one can conclude that the modification of $La_{1-x}Sr_xMnO_3$ manganite nanoparticles, particularly by partial substitutions either in La, or in Mn sublattice, strongly affects their properties. It is shown that the maximal temperature achieved under AC magnetic field depends mainly on the value of the nanoparticles' Curie point. As a result, by changing the phase transition temperature by partial substitution of Mn by another 3*d*-element or La by another rare-earth element, one can provide a rigid control of the maximal temperature achieved upon the action of the AC magnetic field. This, in turn, means that manganite nanoparticles doped with other elements are promising materials to be used as the mediators of self-controlled magnetic nanohyperthermia.

4. Conclusions

Magnetostatic properties and AC magnetic heating characteristics of manganite nanoparticles with substitutions in manganese and lanthanum sublattices synthesized via sol–gel method have been studied. It is shown that the increase in doping element (Fe or Sm) results in lowering Curie temperature and weakening heating efficiency under the action of AC magnetic field. It follows from the experiments that the substitutions in Mn sublattice result in more rapid changes of magnetic parameters, as compared to the substitutions in La one. The results demonstrate that the action of external magnetic field causes the effective heating of nanoparticles at temperatures lower than T_C. Thus, fine tuning of the Curie temperature of nanoparticles allows controlling the maximal temperature achieved during the heating.

Acknowledgments

The work is partially supported by the Ministry of Education and Science of Ukraine through the project "Micro- and nanofluidics in stray magnetic fields of artificial and biogenic magnetic particles", project No. 0118U003790.

References

[1] Q.A. Pankhurst, N.T.K. Thanh, S.K. Jones, J. Dobson, *J. Phys. D Appl. Phys.* **42**, 224001 (2009).

[2] S. Hyun Noh, S.H. Moon, T.H. Shin, Y. Lim, J. Cheon, *Nano Today* **13**, 61 (2017).

[3] E.A. Perigo, G. Hemery, O. Sandre, D. Ortega, E. Garaio, F. Plazaola, F.J. Teran, *Appl. Phys. Rev.* **2**, 041302 (2015).

[4] A.A. Kuznetsov, O.A. Shlyakhtin, N.A. Brusentsov, O.A. Kuznetsov, *Eur. Cells Mater.* **3**, 75 (2002).

[5] N.K. Prasad, K. Rathinasamy, D. Panda, D. Bahadur, *J. Biomed. Mater. Res. B Appl. Biomater.* **85**, 409 (2008).

[6] E. Pollert, K. Knížek, M. Maryško, P. Kašpar, S. Vasseur, E. Duguet, *J. Magn. Magn. Mater.* **316**, 122 (2007).

[7] O. Kaman, T. Dědourková, J. Koktan, J. Kuličková, M. Maryško, P. Veverka, R. Havelek, K. Královec, K. Turnovcová, P. Jendelová, A. Schröfel, L. Svoboda, *J. Nanoparticle Res.* **18**, 100 (2016).

[8] A. ur Rashid, S. Manzoor, *J. Magn. Magn. Mater.* **420**, 232 (2016).

[9] A.G. Belous, O.I. V'yunov, E.V. Pashkova, O.Z. Yanchevskii, A.I. Tovstolytkin, A.M. Pogorelyi, *Inorg. Mater.* **39**, 161 (2003).

[10] K. Zhang, T. Holloway, J. Pradhan, M. Bahoura, R. Bah, R.R. Rakhimov, A.K. Pradhan, R. Prabakaran, G.T. Ramesh, *J. Nanosci. Nanotechnol.* **10**, 5520 (2010).

[11] D.H. Manh, P.T. Phong, P.H. Nam, D.K. Tung, N.X. Phuc, I.J. Lee, *Phys. B Condens. Matter* **444**, 94 (2014).

[12] J.R. Sun, G.H. Rao, B.G. Shen, H.K. Wong, *Appl. Phys. Lett.* **73**, 2998 (1998).

[13] K. Ghosh, S. Ogale, R. Ramesh, R. Greene, T. Venkatesan, K. Gapchup, R. Bathe, S. Patil, *Phys. Rev. B* **59**, 533 (1999).

[14] Y. Shlapa, S. Solopan, A. Bodnaruk, M. Kulyk, V. Kalita, Y. Tykhonenko-Polishchuk, A. Tovstolytkin, A. Belous, *Nanoscale Res. Lett.* **12**, 100 (2017).

[15] J.R. Sun, G.H. Rao, J.K. Liang, *Appl. Phys. Lett.* **70**, 1900 (1997).

[16] A.G. Belous, S.O. Solopan, O.V. Yelenich, A.I. Tovstolytkin, T.V. Kolodiazhnyi, S.P. Osinsky, L.N. Bubnovskaya, *AIP Conf. Proc.* **1627**, 13 (2014).

[17] Y. Shlapa, M. Kulyk, V. Kalita, T. Polek, A. Tovstolytkin, J.-M. Greneche, S. Solopan, A. Belous, *Nanoscale Res. Lett.* **11**, 24 (2016).

[18] Y. Shlapa, S. Solopan, A. Bodnaruk, M. Kulyk, V. Kalita, Y. Tykhonenko-Polishchuk, A. Tovstolytkin, V. Zinchenko, A. Belous, *J. Alloys Comp.* **702**, 31 (2017).

[19] L. Bubnovskaya, A. Belous, S. Solopan, A. Kovelskaya, L. Bovkun, A. Podoltsev, I. Kondtratenko, S. Osinsky, *J. Nanopart.* **2014**, 1 (2014).

[20] E. Dagotto, T. Hotta, A. Moreo, *Phys. Rep.* **344**, 1 (2001).

[21] O.Z. Yanchevskii, O.I. V'yunov, A.G. Belous, A.I. Tovstolytkin, *Low Temp. Phys.* **32**, 134 (2006).

[22] K. Dörr, *J. Phys. D. Appl. Phys.* **39**, R125 (2006).

[23] J. Carrey, B. Mehdaoui, M. Respaud, *J. Appl. Phys.* **109**, 083921 (2011).

[24] V.M. Kalita, A.I. Tovstolytkin, S.M. Ryabchenko, O.V. Yelenich, S.O. Solopan, A.G. Belous, *Phys. Chem. Chem. Phys.* **17**, 18087 (2015).